Local adsorption geometry of acetylene on Si(100)(2×1)

R. Terborg, P. Baumgärtel, R. Lindsay, O. Schaff, T. Gießel, J. T. Hoeft, and M. Polcik
Fritz-Haber-Institut der Max-Planck-Gesellschaft, Faradayweg 4-6, 14195 Berlin, Germany

R. L. Toomes
Department of Physics, University of Warwick, Coventry CV4 7AL, Great Britain

S. Kulkarni
Fritz-Haber-Institut der Max-Planck-Gesellschaft, Faradayweg 4-6, 14195 Berlin, Germany
and Physics Department, University of Pune, Poona 411007, Maharashtra, India

A. M. Bradshaw
Fritz-Haber-Institut der Max-Planck-Gesellschaft, Faradayweg 4-6, 14195 Berlin, Germany

D. P. Woodruff*
Department of Physics, University of Warwick, Coventry CV4 7AL, Great Britain
(Received 13 January 2000)

Using C 1*s* scanned-energy-mode photoelectron diffraction the local adsorption geometry of acetylene on the Si(100)(2×1) surface has been determined and the results are compared with those of a similar study of ethylene adsorption on this surface. Both molecules bond to the surface along the Si-Si dimers with the C-C bonds parallel to the surface such that the C atoms are in off-atop sites relative to the Si dimer atoms. In both cases the Si-Si bond length (2.36±0.21 Å for ethylene and 2.44±0.58 Å for acetylene) is compatible only with the dimer remaining intact after adsorption and not with the Si-Si distance of an ideally terminated undimerized Si(100) surface (3.84 Å).

I. INTRODUCTION

In the last few years there has been growing interest in the adsorption of organic molecules onto Si surfaces with a view to developing a practical methodology to exploit molecular electronics. The interaction of small unsaturated hydrocarbon molecules on Si(100) provides a simple model system to explore the relevant underlying physics and chemistry.[1] The clean Si(100) surface is known to reconstruct, the key process being the production of Si-Si dimers at the surface, nominally reducing the number of dangling bonds per surface Si atom from two on an ideally terminated surface to one on a fully dimerized surface. At room temperature one observes a (2×1) reconstruction,[2] which is now generally agreed to involve actual dynamical ''flipping'' of asymmetric dimers[3] arranged on a (2×1) mesh rather than a true long-range-ordered (2×1) phase; at low temperatures ordering of the asymmetric dimers results in a $c(4\times2)$ phase.[4]

Using a range of experimental spectroscopies and real-space imaging with the scanning tunneling microscope[5–19] as well as total-energy calculations (both *ab initio*[20–25] and semiempirical)[26–32] there is a general consensus that ethylene $H_2C{=}CH_2$ and acetylene $HC{\equiv}CH$ both bond to the Si(100) surface along the Si-Si dimers in a so-called *di-σ* configuration. Most studies indicate that the Si-Si dimers remain intact and probably become essentially symmetric (with the Si-Si and C-C bonds parallel to the surface—see Fig. 1), although there have been both experimental and theoretical results that have been taken to indicate fracture of the Si-Si dimers for both ethylene[11,12,14,15,29] and acetylene[10,13,30] adsorption.

In order to obtain quantitative structural information we have applied the scanned-energy-mode photoelectron diffraction (PhD) experimental technique[33] to these two adsorption systems. This method exploits the coherent interference between the directly emitted component of the photoelectron wave field from a core level of an adsorbed atom with the components of the same wave field elastically scattered by the surrounding (mainly substrate) atoms. This interference gives rise to modulations in the photoelectron

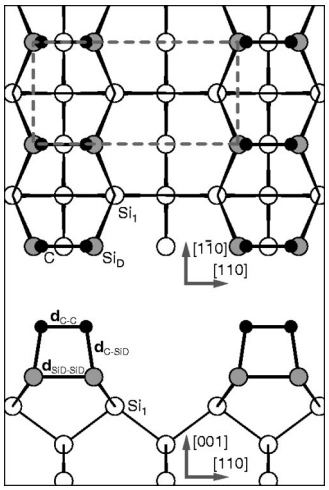

FIG. 1. Schematic diagram of adsorbed C_2H_2 or C_2H_4 on Si(100) with the molecule bonding to symmetric Si-Si dimers in a (2×1) phase; the key local structural parameters are defined. The H atoms are not shown.

intensity measured in any specific emission direction as the photoelectron energy (and thus wavelength) changes and the scattering paths move in and out of phase. An integrated experimental and theoretical modeling PhD methodology[33,34] has been developed and applied to the successful quantitative structure determination of some 50 or more adsorption systems. The detailed results of our PhD study of the Si(100)/ethylene adsorption system provide clear confirmation that the adsorption does occur at symmetric but intact Si-Si dimers and have recently been presented elsewhere.[35] Here we present the results of a similar study of acetylene adsorption on Si(100)(2×1) and compare these with the ethylene adsorption results. Comparison of the PhD data also provides a clearer understanding of the relatively poor precision of our structure determination for acetylene adsorption.

II. EXPERIMENTAL DETAILS

The experiments were conducted at the BESSY I synchrotron radiation facility in Berlin on the HE-TGM-1 beam line.[36] The UHV end-station chamber is fitted with low-energy electron diffraction (LEED) optics and a concentric spherical sector electron spectrometer (VG Scientific, 152 mm radius, three-channeltron detector) for soft x-ray photoelectron spectroscopy (SXPS), the latter being used both to characterize the surface cleanness and to measure the photoelectron diffraction spectra. The 0.5-mm-thick Si(100) wafer (P doped, 10 Ω cm), cleaved to a rectangle of 12×7 mm,^{2} was rinsed in methanol and ultrapure water prior to mounting on the UHV manipulator fitted with direct current heating together with cooling from a liquid-helium reservoir connected by copper braid to one of the metal clips of the sample mounting. The sample was cleaned *in situ* by flashing to 1520 K, yielding a surface showing a well-ordered two-domain (2×1) LEED pattern at room temperature with no detectable contamination seen in SXPS. All measurements were made with the sample cooled. In the case of the ethylene adsorption, cooling was with liquid helium; the temperature reading at the metallic clip holding the sample was typically 60 K, although the true sample temperature is likely to be slightly higher than this. When cold the clean surface showed a two-domain $c(4\times2)$ LEED pattern, clearly indicating a sample temperature below about 200 K,[4] and probably very much lower.

For the acetylene work liquid-nitrogen cooling was used leading to a sample thermocouple reading of 100 K. The sample was exposed at low temperature to either ethylene or acetylene to exposures of 2×10^{-5} mbar s; on the basis of the C 1*s* peak intensity in SXPS after successive doses, this appeared to yield saturation coverages. Following these exposures the LEED pattern changed to one characteristic of two orthogonal domains of a (2×1) unit mesh. As discussed by other authors previously, this is most probably due to removal of the asymmetry of the long-range-ordered $c(4\times2)$ alternately inclined dimers, which gives rise to the smaller unit mesh.

For each adsorbate system the C 1*s* photoelectron diffraction data were measured in the kinetic energy range 100–470 eV in the two main azimuthal directions ⟨100⟩ and ⟨110⟩ for polar emission angles between 0° and 60° in steps of 10° with additional measurements at 15° in the case of ethylene adsorption. The photon energy was incremented in steps of 2 eV to cover the necessary kinetic energy range for the C 1*s* photoelectrons, and at each photon energy the emitted electron signal was recorded, in the kinetic energy range of ±25 eV around the C 1*s* core-level peak, to give a series of energy distribution curves (EDCs). The intensity of the peak in each EDC was then determined by background subtraction and integration, and the resulting intensity-energy spectra were normalized to give the photoelectron diffraction modulation functions. The modulation function is defined by

$$\chi_{\mathrm{ex}}(\theta,\phi,k)=[I(k)-I_0(k)]/I_0(k), \tag{1}$$

where $I(k)$ and $I_0(k)$ are the diffractive and nondiffractive intensities, θ and ϕ are the polar and azimuthal emission angles, and k is the modulus of the photoelectron wave vector. $I_0(k)$ also includes the influence of smoothly varying instrumental effects and is obtained by performing a smooth fit to $I(k)$ with a spline function. The data sets chosen for the subsequent structure determinations comprised nine such modulation functions from adsorbed ethylene and six from acetylene, and these are shown as the bold curves in Fig. 2.

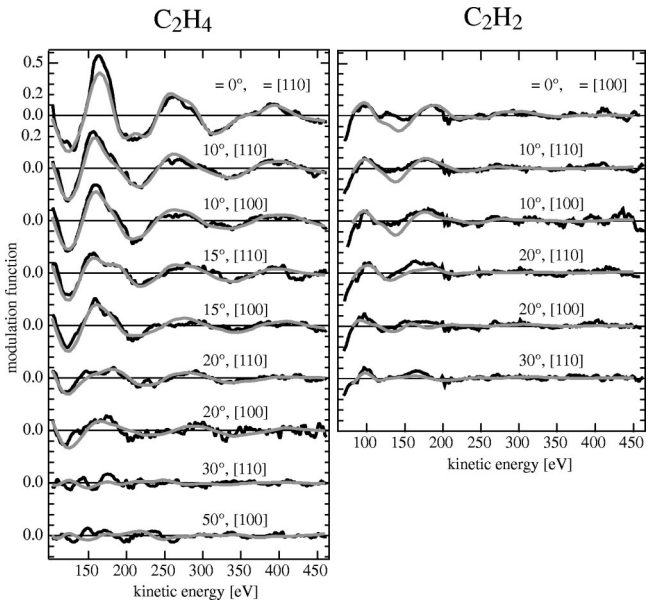

FIG. 2. Comparison of experimental (bold lines) and theoretically simulated (gray lines) C 1*s* PhD spectra from ethylene and acetylene adsorbed on Si(100)(2×1).

III. RESULTS AND DATA ANALYSIS

Our integrated approach[34] to the analysis of PhD data and the associated structure analysis typically involves two stages. In the first, application of a direct method of data inversion to produce an approximate ''image'' of the local scatterer environment of the emitter atoms provides a first-order assignment of the local adsorption site. In the second, the results of multiple-scattering simulations for model structures are compared directly with the experimental data and the structural parameters of the model adjusted to optimize the agreement between theory and experiment.

For the first stage of direct data inversion we use the so-called projection method.[37,38] The underlying physical

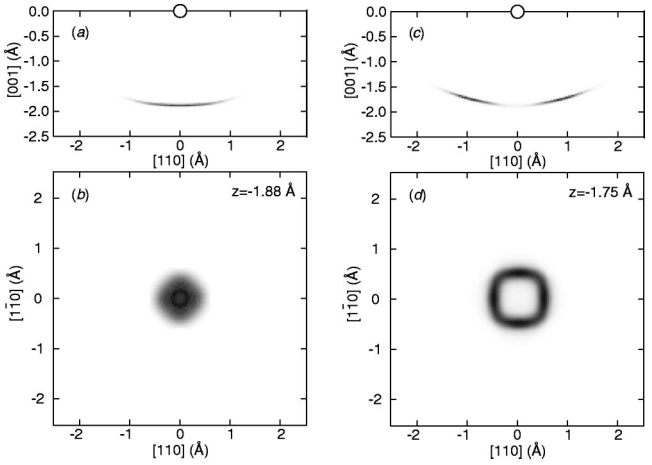

FIG. 3. Results of applying the projection method of direct data inversion to the experimental photoelectron diffraction spectra of Fig. 2. The projection method provides a three-dimensional image of the surroundings of the emitter [located at (0, 0, 0)], the parameter mapped having the highest intensity at locations most likely to correspond to those of near-neighbor backscatterers. (a) and (b) show gray-scale mapping of this parameter in a plane perpendicular to the surface passing through the C emitter of ethylene and acetylene, respectively, in a ⟨110⟩ azimuth. (b) and (d) show similar maps in planes parallel to the surface cutting through the dominant features of (a) and (b) at depths of 1.88 and 1.75 Å below the emitter.

principle is that modulation functions measured in directions that correspond to 180° scattering from a near-neighbor substrate atom are typically dominated by interference from this one scattering path and show particularly strong intensity modulations. This modulation function can thus be described reasonably well within the single-scattering approximation from this one scatterer. The method involves the calculation of integrals of the actual experimental spectra projected onto such calculated spectra based on this simple single-scattering description and produces a three-dimensional intensity map of the space around the emitter, with maximum values of the projection integral in regions corresponding to the most probable locations of nearest-neighbor backscatterers. Notice that a key aspect of this approach is the reliance on geometries involving a single dominant backscattering event, which in turn implies an emitter (adsorption) site at, or close to, a site of high symmetry. The results of applying this approach to the present experimental data sets are shown in Fig. 3. The projection method provides a three-dimensional image of the surroundings of the emitter with the parameter mapped having the highest intensity at locations most likely to correspond to those of near-neighbor backscatterers. This parameter is shown in a gray-scale mapping for sections perpendicular to the surface passing through the emitter in the upper panels of Fig. 3. In both of these upper panels one sees a saucerlike feature approximately 1.8 Å directly below the emitter; the shape of these features results from the form of the contours of constant path-length difference for a near-neighbor scatterer. In the lower panels are seen similar maps taken in planes parallel to the surface but below the emitter by a distance determined by the location of the peak in the upper panels. In the case of the ethylene data inversion, this surface-parallel cut shows a broad feature centered around the position directly below the emitter, but actually peaks around a ring or radius some 0.2 Å around this point. This ring effect is much more pronounced for acetylene, for which the ring radius is 0.5–0.6 Å. The most obvious interpretation of these images is that in both adsorption systems the C emitter atoms lie slightly off-atop a surface Si atom, with the offset being larger for acetylene. Notice that the projection maps incorporate the full symmetry of the substrate, as will be imposed on the PhD data, so even if the true offset were in ⟨100⟩ or ⟨110⟩ azimuths only, the parallel maps would show four symmetrically positioned features around the center. The fact that rings are seen may be due to some combination of the obvious smearing or poor resolution of the images and possible components of the offset out of one of these high-symmetry azimuths.

The essential indication of off-atop geometries for the C emitter atoms is consistent with our expectation of molecular adsorption parallel to the Si-Si dimers. On a clean Si(100) surface the Si-Si dimer bond lengths found in theoretical calculations are typically around 2.3 Å, whereas the C-C bond lengths in gas-phase ethylene and acetylene are 1.33 and 1.21 Å, respectively, so while all of these distances may be modified by the adsorbate-surface bonding, it is clear that there is unlikely to be a match of the Si-Si and C-C distances, forcing the C atoms into off-atop sites.

The second stage of our PhD structure determination methodology is a full quantitative structural analysis using an iterative ''trial-and-error'' procedure comparing a set of experimental spectra with the results of multiple-scattering simulations based on trial model structures. These calculations use computer codes developed by Fritzsche[39–41] based on the expansion of the final-state wave function into a sum over all electron scattering pathways from the emitter atom to the detector outside the sample. A magnetic quantum number expansion of the free-electron propagator is used to calculate the scattering contribution of an individual scattering path. Double- and higher-order scattering events are treated by means of the reduced angular momentum expansion. The influence of the finite energy resolution and angular acceptance of the electron analyzer, both of which improve convergence, is included. In order to quantify the level of agreement between theory and experiment, a reliability factor or R factor is defined as[42]

$$R_m = \sum (\chi_{\text{theor}} - \chi_{\text{expt}})^2 \Big/ \sum (\chi^2_{\text{theor}} + \chi^2_{\text{expt}}), \qquad (2)$$

where a value of 0 corresponds to perfect agreement, a value of 1 to uncorrelated data, and a value of 2 to anticorrelated data. In order to establish the significance of best fits to different structural models and to estimate the precision associated with the individual structural parameters we use an approach based on that of Pendry, which was derived for LEED.[43] This involves defining a variance in the minimum of the R factor, $R_{\min}$, as

$$\text{Var} = R_{\min}\sqrt{2/N}, \qquad (3)$$

where N is the number of independent pieces of structural information contained in the set of modulation functions used in the analysis. Structures and parameter values leading to R factors less than $R_{\min} + \text{Var}(R_{\min})$ are regarded as falling

TABLE I. Best-fit parameter values obtained in this work for the local geometry of adsorbed acetylene and ethylene on Si(100)(2×1).

Parameter	Si(100)(2×1)-C_2H_2	Si(100)(2×1)-C_2H_4
$d_{C\text{-}C}$	1.36±0.19 Å	1.62±0.08 Å
$d_{C\text{-}SiD}$	1.83±0.04 Å	1.90±0.01 Å
∠C-C-SiD	(107±9)°	(101±3)°
$d_{SiD\text{-}SiD}$	2.44±0.58 Å	2.36±0.21 Å
$z_{C\text{-}Si1}$	2.78±0.25 Å	2.81±0.18 Å
$z_{C\text{-}Si2}$	4.55−1.42/+∞ Å	4.41±0.17 Å
$\phi_{C\text{-}C}$	(0±23)°	(0±13)°

within one standard deviation of the best-fit structure. More details of this approach and the definition of *N* can be found elsewhere.[44] Note that in applying this approach to estimate the precision in multiparameter structural fits in a variety of different techniques, it is common to consider changes in the *R* factor produced by changing each parameter separately. This procedure, however, takes no account of possible coupling between parameters whereby the degradation in fit produced by a change in one parameter can be overcome by a change in a second parameter. We have recently described a general method for investigating this effect in PhD using a Hessian matrix approach;[45] a very similar approach has previously been proposed for use in LEED.[46] Using this approach we have checked for such coupling of parameter errors, and the precision values quoted here are essentially worst-case estimates that take into account this problem.[45]

Full details of the optimization of the structural model for ethylene adsorption on Si(100)(2×1) on the basis of the data for this system shown in Fig. 2 have already been presented elsewhere,[35] but the key result is that the molecule is found to bond with the C-C axis parallel to the surface, symmetrically positioned over symmetric Si-Si dimers, with a C-C distance of 1.62±0.08 Å, a Si-Si dimer bond length of 2.36±0.21 Å, and a C-Si distance of 1.90±0.01 Å. This places the O atoms in sites displaced parallel to the surface along the dimer directions by 0.37 Å off atop. The full set of optimized structural parameter values is summarized in Table I, which also includes the precision with which any possible azimuthal twist of the C-C axis about the surface normal ($\phi_{C\text{-}C}$) can be excluded.

Before discussing the application of a similar structural optimization to the case of acetylene on Si(100), however, it is helpful to draw some general conclusions from comparison of the PhD modulation spectra from ethylene and acetylene adsorption. One very striking feature of a comparison of the actual PhD spectra, as shown in Fig. 2, is the very weak modulations seen in the acetylene data. The ethylene PhD spectra seen in Fig. 2 are rather typical of such data from an adsorbate emitter in a near-atop geometry. Reasonably strong (±40% at low energy) modulations are seen at normal emission, with a single dominant periodicity, indicative of a single dominant scattering path involving close to 180° scattering from the nearest-neighbor Si atom below. The amplitude of these modulations falls as the polar emission angle increases to only about 10% at 20°, and there is no strong scattering reappearing at large polar angles. The failure to see strong 180° backscattering from non-nearest-neighbor outermost layer substrate atoms is rather typical of PhD data from atop adsorbed species and has been attributed to relatively large-amplitude frustrated translational vibrational modes parallel to the surface (e.g., for CO,[47] PF_3,[42] and[44] NH_3.) In the present case such vibrations may also play a role, but the fact that the emitter is off atop will also lead to this result; summing over the symmetrically equivalent off-atop static positions will have a very similar effect to summing over a dynamical distribution of positions about the atop site produced by vibrations. In the case of the Si(100) surface the relatively large Si-Si spacings on the surface and the reduced symmetry of the dimer must contribute to this effect. Indeed, very similar results were found in N 1*s* PhD from NH_2 on Si(100)(2×1), which occupies an off-atop site.[48]

In the case of the acetylene adsorption, however, the C 1*s* PhD modulations are only around 10–15 % at normal emission, yet still fall to even smaller values at increasing polar emission angles. The direct inversion of these data, shown in Fig. 3, provides some hint as to why this may be the case, in that this appears to indicate that the C adsorption sites are more strongly displaced from the favored atop sites. This does, indeed, prove to be the case. The best-fit structure for acetylene on Si(100) places the molecule in the same symmetric configuration as for ethylene, but a reduced C-C bond length and an increased Si-Si bond length combine to increase the offset of the emitter and scatterer parallel to the surface, while a reduction in the C-Si distance also serves to increase the C-C-Si angle and thus shift the nearest-neighbor Si scattering angle in normal emission even further from the favored value of 180° (see Table I). Notice, however, that because the PhD modulations are so weak in all the acetylene spectra, the precision with which these structural parameters can be determined is very much worse than for ethylene. This arises from the high value of the *R* factor for the best-fit structure (a rather poor value of 0.40 for acetylene compared with an exceptionally low value of 0.057 for ethylene). The *R* factor is defined as being a sum of square deviations between theory and experiment, but it is normalized by the actual values of these two quantities. This means that a discrepancy of, say, 2% in the modulation amplitude has a far greater effect on the *R*-factor value if the average modulation is weak (say 10%) than if it is strong (say 30–40 %). The actual discrepancies, of course, are attributable to both experimental noise and limitations in the theoretical and computational description, but the evidence of many previous studies is that providing one can identify a number of emission directions in which strong modulations are seen, neither of these deficiencies presents a significant limitation to the method. If only weak modulations are seen, this is no longer the case.

If we compare the two experimental data sets for the subset of emission geometries common to both, using the same *R* factor normally used for comparing experiment and theory, we obtain a value of 0.80, clearly indicating the marked difference between these spectra that is seen on visual inspection. In order to understand the difference between the two sets of PhD spectra shown in Fig. 2 in more detail, some further test calculations were conducted comparing the experimental data from adsorbed acetylene with models which started with that found to describe the ethylene results and

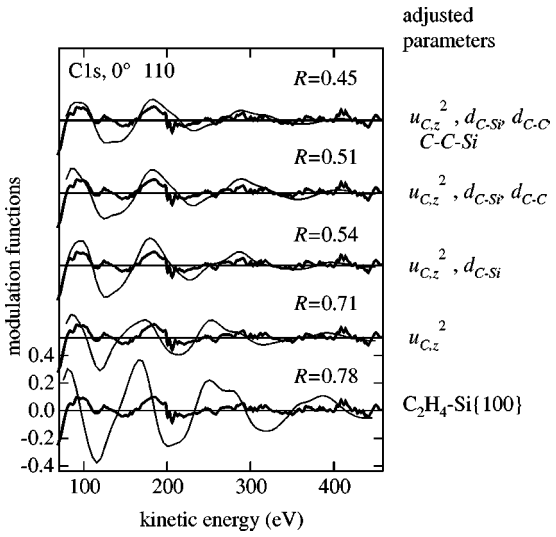

FIG. 4. Comparison of the experimental normal emission C 1*s* PhD spectrum from adsorbed acetylene on Si(100)(2×1) with theoretical simulations in which the structural parameters appropriate to adsorbed ethylene (Table I) are replaced one at a time by the best-fit values for adsorbed acetylene (see also Table I). The *R*-factor values shown correspond to the values for the full set of experimental spectra used in the analysis (Fig. 2) and not just the normal emission spectrum shown here.

then replaced the key parameter differences between the two systems (Table I) individually. The results of this exercise are shown, for the normal emission spectrum only, in Fig. 4. Comparison of the theoretical spectra for ethylene geometry with the experimental acetylene data yields an *R* factor of 0.78; the fact that this value is almost identical to that obtained by comparing the two experimental data sets reflects the fact that the differences between theory and experiment for the ethylene data are small compared with the differences between the two adsorbates. As may be seen in Fig. 4, the theoretical simulation of the normal emission spectrum for the ethylene geometry not only shows much stronger modulations than seen in the experimental acetylene spectrum, but also shows energy shifts in the peak positions, implying a change in the length of the dominant scattering path-length difference. While Table I compares the static optimum structural parameters of the two systems, one other fitting parameter, the mean-square vibrational amplitude of the C emitter perpendicular to the surface, differs significantly in the two fits. In particular, this value was found to be $0.003 \pm 0.002\,\text{Å}^2$ for ethylene and $0.010 \pm 0.007\,\text{Å}^2$ for acetylene. This difference may, in part, be due to the higher temperature (100 K) at which the acetylene data were recorded relative to that used for ethylene (60 K). Notice that the fitting procedure for both data sets allowed for different vibrational amplitudes of the emitter in each of the orthogonal directions in the surface and perpendicular to the surface, and also allowed the nearest-neighbor Si atoms to the emitters to have different vibrational amplitudes from the bulk Si atoms, in order to take some account of correlated vibrations. The vibrational amplitude of the emitter atoms perpendicular to the surface was the one that changed most between the two adsorbate systems, but while this larger vibrational amplitude in the case of acetylene leads to some attenuation of the PhD modulations as seen in Fig. 4, if *only* this parameter is adjusted in the ethylene geometry, the fit to the experimental acetylene data is still very poor (*R* factor value of 0.71). Changing both this vibrational amplitude and the distance of the C emitter to the nearest-neighbor Si(dimer) atom, $d_{\text{C-SiD}}$, leads to a more significant improvement to an *R* value of 0.54, while additionally changing the C-C distance ($d_{\text{C-C}}$), and subsequently the C-C-Si(dimer) bond angle [and hence the Si-Si(dimer) bond length, $d_{\text{SiD-SiD}}$], further lowers *R* to 0.51 and finally to 0.45. Evidently the improved modulation amplitude arising from the enhanced vibrations is significant, but the larger *R*-factor improvements arise from the changes in bond lengths and associated bond angles. Optimization of the remaining parameters involves smaller changes in individual parameters but reduces the overall *R*-factor value to 0.40, with an associated variance of 0.07. This means that the fit immediately prior to this final optimization lies within the final value of $R_{\min}$ plus its variance (0.47), but all the others lie outside the variance.

IV. DISCUSSION AND CONCLUSIONS

The primary structural information arising from this work is summarized in Table I. Two significant conclusions may be drawn from these parameter values. First, both ethylene and acetylene are found to bond parallel to the surface and are symmetrically located above symmetric Si dimers. Secondly, these Si dimers are intact; even in the case of the very low precision in the Si-Si dimer bond length obtained in the case of adsorbed acetylene, the value obtained ($2.44 \pm 0.58\,\text{Å}$) is clearly incompatible with the Si-Si distance on an ideally truncated (nondimerized) Si(100) surface (3.84 Å). The issue of whether or not the adsorption of these species breaks the dimer bond has been controversial, and while recent *ab initio* theoretical treatments have certainly favored intact dimers, our results provide a quantitative experimental demonstration of this conclusion.

A more detailed quantitative comparison of the structural parameters we derive from our experiments with the results of total-energy calculations is contained in Table II. A number of general trends are clear. First, the theoretical values of the C-C bond lengths, with only one exception, show the values for adsorbed acetylene around 1.32–1.37 Å and adsorbed ethylene around 1.50–1.53 Å. These values are consistent with those corresponding to bond orders of 2 and 1, respectively, as found in gas-phase ethylene (1.33 Å) and ethane (1.53 Å), and imply that the bonding to the Si has reduced the C-C bond order by 1. Our experimental results are consistent with this picture. In the case of adsorbed ethylene our best-fit value is actually longer than this expectation, but the estimated precision indicates that a bond order of 1 is reasonable but a higher integral value is not. In the case of adsorbed acetylene, our experimental C-C distance is consistent with the expected bond order of 2, although the low precision renders this bond-order determination formally not significant. Secondly, the Si-Si dimer bond length shown in the calculations shows no obvious consistent trend that distinguishes the two different adsorbates, and our optimum experimental values in the presence of the two adsorbates agree to an extent that is much smaller than the estimated imprecision. The key result here is simply that the dimer is intact, with a bond length consistent with expectations. Com-

TABLE II. Comparison of structural parameter values from this work (expt) and from various theoretical calculations for ethylene and acetylene adsorbed on Si(100)(2×1).

	C_2H_2							C_2H_4			
	(expt)	Ref. 22	Ref. 21	Ref. 31	Ref. 25	Ref. 26	Ref. 27	(expt)	Ref. 23	Ref. 24	Ref. 22
$d_{C\text{-}C}$ (Å)	1.36±0.19	1.37	1.36	1.49	1.40	1.33	1.32	1.62±0.08	1.52	1.50	1.53
$d_{SiD\text{-}SiD}$ (Å)	2.44±0.58	2.40	2.36	2.23	2.40	2.23	2.43	2.36±0.21	2.33	2.39	2.39
$d_{C\text{-}SiD}$ (Å)	1.83±0.04		1.90	1.98	1.94	1.87	1.78	1.90±0.01	1.93	2.01	1.95
∠C-C-SiD (°)	107±9	105	105	101	105	104	108	101±3	102	102	103

parison of the C-Si(dimer) bond-length values, however, shows a rather consistent discrepancy between our experimental values and those of the total-energy calculations. Because this bonding direction lies quite close to the surface normal and the backscattering of this nearest-neighbor Si atom dominates the PhD spectra, this distance can be determined rather precisely in our experiments, even in the case of adsorbed acetylene. Our value for adsorbed ethylene is consistently and very significantly smaller than the theoretical values, while a similar trend is seen for adsorbed acetylene, although two of the values from the semiempirical calculations[26,27] do fall within the experimental range. This comparison does suggest a systematic problem in the *ab initio* calculations.

In addition to these structural conclusions, which clearly are the motivation for this work, some comment on the PhD results for adsorbed acetylene appear appropriate. We note, in particular, the poor value of the *R* factor (0.40) for the best-fit structure, which compares unfavorably with values found in other structural studies by this method, which more usually fall below 0.30, and indeed are often below 0.20. The reason for this poor *R* factor, however, can be attributed very directly to the weak PhD modulations that are found even in the near-normal emission direction, which appears to be the most favorable direction for this system. Weak modulations mean that experimental noise and any deficiencies in the theoretical description have a far more serious effect on the *R* factor. However, these weak modulations can be reproduced effectively by the theoretical simulation and do appear to be intrinsic to the system, due to a combination of a low-symmetry adsorption geometry for the individual C atomic emitters and a significant (but not exceptionally large) amplitude of molecular vibration perpendicular to the surface. We should stress, however, that the method of data analysis and evaluation explicitly takes account of the large value of the *R* factor and leads to much reduced precision. This precision has been fully considered in the discussion of the significance of the structural conclusions outlined above.

ACKNOWLEDGMENTS

The authors wish to acknowledge financial support for this work from the German Federal Ministry of Education and Research (BMBF), Contract No. 05 625EBA 6, the Engineering and Physical Sciences Research Council, and the Fonds der Chemischen Industrie. AMB and DPW also thank the Max-Planck-Gesellschaft and the Alexander-von-Humboldt Stiftung for a Max-Planck grant.

*Corresponding author. Electronic address: D.P.Woodruff@Warwick.ac.uk

[1] J. T. Yates, Jr., Science **279**, 335 (1998).
[2] R. E. Schlier and H. E. Farnsworth, J. Chem. Phys. **30**, 917 (1959).
[3] J. Dabrowski and M. Scheffler, Appl. Surf. Sci. **56-58**, 2338 (1993).
[4] T. Tabata, T. Aruga, and Y. Murata, Surf. Sci. **179**, L63 (1987).
[5] M. Nishijima, J. Yoshinobu, H. Tsuda, and M. Onchi, Surf. Sci. **192**, 383 (1987).
[6] J. Yoshinobu, H. Tusda, M. Onchi, and M. Nishijama, J. Chem. Phys. **87**, 7332 (1987).
[7] C. C. Cheng, R. M. Wallace, P. A. Taylor, W. J. Choyke, and J. T. Yates, Jr., Appl. Phys. A: Solids Surf. **67**, 3693 (1990).
[8] C. C. Cheng, W. J. Choyke, and J. T. Yates, Jr., Surf. Sci. **231**, 289 (1990).
[9] J. T. Yates, Jr., J. Phys.: Condens. Matter **3**, S143 (1991).
[10] P. A. Taylor, R. M. Wallace, C. C. Cheng, W. H. Weinberg, M. J. Dresser, W. J. Choyke, and J. T. Yates, Jr., J. Am. Chem. Soc. **114**, 6754 (1992).
[11] L. Clemen, R. M. Wallace, P. A. Taylor, M. J. Dresser, W. J. Choyke, W. H. Weinberg, and J. T. Yates, Jr., Surf. Sci. **268**, 205 (1992).
[12] W. Widdra, C. Huang, G. A. D. Briggs, and W. H. Weinberg, J. Electron Spectrosc. Relat. Phenom. **64/65**, 129 (1993).
[13] C. Huang, W. Widdra, X. S. Wang, and W. H. Weinberg, J. Vac. Sci. Technol. A **11**, 2250 (1993).
[14] C. Huang, W. Widdra, and W. H. Weinberg, Surf. Sci. **315**, L953 (1994).
[15] W. Widdra, C. Huang, and W. H. Weinberg, Surf. Sci. **329**, 295 (1995).
[16] W. Widdra, C. Huang, S. I. Yi, and W. H. Weinberg, J. Chem. Phys. **105**, 5605 (1996).
[17] H. Liu and R. J. Hamers, J. Am. Chem. Soc. **119**, 7593 (1997).
[18] W. Widdra, A. Fink, S. Gokhale, P. Trischberger, D. Menzel, U. Birkenheuer, U. Gutdeutsch, and N. Rosch, Phys. Rev. Lett. **80**, 4269 (1998).
[19] F. Matsui, H. W. Yeom, A. Imanishi, K. Isawa, I. Matsuda, and T. Ohta, Surf. Sci. **401**, L413 (1998).
[20] K. Feng, Z. H. Liu, and Z. Lin, Surf. Sci. **329**, 77 (1995).
[21] Y. Imamura, Y. Morikawa, T. Yamasaki, and H. Nakatsuji, Surf. Sci. **341**, L1091 (1995).
[22] A. J. Fisher, P. E. Blöchl, and G. A. D. Briggs, Surf. Sci. **374**, 298 (1997); additional parameter values from this work are given in G. A. D. Briggs and A. J. Fisher, Surf. Sci. Rep. **33**, 1 (1999).

[23] W. Pan, T. Zhu, and W. Yang, J. Chem. Phys. **107**, 3981 (1997).
[24] U. Birkenheuer, U. Gutdeutsch, N. Rösch, A. Fink, S. Gokhale, D. Menzel, P. Trischberger, and W. Widdra, J. Chem. Phys. **108**, 9868 (1998).
[25] B. Meng, D. Maroudas, and W. H. Weinberg, Chem. Phys. Lett. **278**, 97 (1997).
[26] Q. Liu and R. Hoffmann, J. Am. Chem. Soc. **117**, 4082 (1995).
[27] B. I. Craig and P. V. Smith, Surf. Sci. **276**, 174 (1992).
[28] B. I. Craig and P. V. Smith, Surf. Sci. **285**, 295 (1993).
[29] B. I. Craig, Surf. Sci. **329**, 293 (1995).
[30] C. S. Carmer, B. Weiner, and M. Frenklach, J. Chem. Phys. **99**, 1356 (1993).
[31] R. H. Zhou, P. L. Cao, and L. Q. Lee, Phys. Rev. B **47**, 10 601 (1995).
[32] P. L. Cao and R. H. Zhou, J. Phys.: Condens. Matter **5**, 2887 (1993).
[33] D. P. Woodruff and A. M. Bradshaw, Rep. Prog. Phys. **57**, 1029 (1994).
[34] D. P. Woodruff, R. Davis, N. A. Booth, A. M. Bradshaw, C. J. Hirschmugl, K.-M. Schindler, O. Schaff, V. Fernandez, A. Theobald, Ph. Hofmann, and V. Fritzsche Surf. Sci. **357/358**, 19 (1996).
[35] P. Baumgärtel, R. Lindsay, O. Schaff, T. Gießel, R. Terborg, J. T. Hoeft, M. Polcik, A. M. Bradshaw, M. Carbone, M. N. Piancastelli, R. Zanoni, R. L. Toomes, and D. P. Woodruff, New J. Phys **1**, 20.1 (1999).
[36] E. Dietz, W. Braun, A. M. Bradshaw, and R. Johnson, Nucl. Instrum. Methods Phys. Res. A **239**, 359 (1985).
[37] Ph. Hofmann and K.-M. Schindler, Phys. Rev. B **47**, 13 941 (1993).
[38] Ph. Hofmann, K.-M. Schindler, S. Bao, A. M. Bradshaw, and D. P. Woodruff, Nature (London) **368**, 131 (1994).
[39] V. Fritzsche, J. Phys.: Condens. Matter **2**, 1413 (1990).
[40] V. Fritzsche, Surf. Sci. **265**, 187 (1992).
[41] V. Fritzsche, Surf. Sci. **213**, 648 (1986).
[42] R. Dippel, K.-U. Weiss, K.-M. Schindler, P. Gardner, V. Fritzsche, P. Gardner, A. M. Bradshaw, M. C. Asensio, X. M. Hu, D. P. Woodruff, and A. R. González-Elipe, Chem. Phys. Lett. **199**, 625 (1992).
[43] J. B. Pendry, J. Phys. C **13**, 937 (1980).
[44] N. A. Booth, R. Davis, R. Toomes, D. P. Woodruff, C. Hirschmugl, K.-M. Schindler, O. Schaff, V. Fernandez, A. Theobald, Ph. Hofmann, R. Lindsay, T. Gießel, and A. M. Bradshaw, Surf. Sci. **387**, 152 (1997).
[45] R. Terborg, J. T. Hoeft, M. Polcik, R. Lindsay, O. Schaff, A. M. Bradshaw, R. L. Toomes, N. A. Booth, D. P. Woodruff, E. Rotenberg, and J. Denlinger, Surf. Sci. **446**, 301 (2000).
[46] J. N. Andersen, H. B. Nielsen, L. Petersen, and D. L. Adams, J. Phys. C **17**, 173 (1984).
[47] Ph. Hofmann, K.-M. Schindler, S. Bao, V. Fritzsche, A. M. Bradshaw, and D. P. Woodruff, Surf. Sci. **337**, 169 (1995).
[48] N. Franco, J. Avila, M. E. Davila, M. C. Asensio, D. P. Woodruff, O. Schaff, V. Fernandez, K.-M. Schindler, V. Fritzsche, and A. M. Bradshaw, Phys. Rev. Lett. **79**, 673 (1997).